

An efficient indoor positioning particle filter using a floor-plan based proposal distribution

Henri Nurminen, Matti Raitoharju, and Robert Piché

Department of Automation Science and Engineering

Tampere University of Technology

Tampere, Finland

Emails: {henri.nurminen, matti.raitoharju, robert.piche}@tut.fi

Abstract—We present a novel floor-plan and PDR (pedestrian dead reckoning) based proposal distribution for indoor positioning particle filtering. Including floor-plan information in the proposal distribution makes the particle filtering more efficient than using the map only in the measurement model, because the proposal distribution becomes more accurate and the measurement model less accurate. The method uses offline-computed distances from each point of a regular grid to the closest wall in each direction. Our simulations show that the novel proposal distribution combined with a floor-plan and PDR based motion model improves the positioning accuracy with small numbers of particles and noisy PDR compared to the particle filters that use the floor-plan only for particle weighting.

I. INTRODUCTION

Wireless network based positioning is an attractive indoor positioning technology due to relatively low costs and wide coverage of wireless communication networks. However, the accuracy is limited by complicated radio environments with details too numerous to be modelled and stored into databases. Therefore, wireless network based measurements are typically complemented with other measurements such as inertial measurements, barometers, and map information, i.e. floor-plan. This article proposes a novel particle filter (PF) algorithm that uses the floor-plan information with improved computational efficiency. Our PF fuses radio positioning, inertial measurement based pedestrian dead reckoning (PDR), and floor-plans.

We formulate indoor positioning as a Bayesian filtering problem that consists of a motion model (dynamical model, state evolution model) and a measurement model. Indoor map measurements are highly non-linear and non-Gaussian, so their application with the Kalman filter (KF), a conventional computationally light and easy-to-implement estimation algorithm, is challenging, and the KF can only use part of the information. Therefore, computationally more challenging methods such as grid filters [1] and PFs [2] have attracted interest in indoor positioning community.

The PF is a Monte Carlo based time series estimation algorithm that generates weighted pseudo-random samples (aka particles) of the state's posterior probability distribution

[3, Ch. 3] [4]. The algorithm is very flexible in the sense that the assumptions of the dynamic and measurement models are not restrictive; in particular, Gaussianity of errors or linearity of models is not required. As the number of particles is increased, the PF solution approaches the minimum mean-square error solution for the given statistical model. However, for some models the number of particles required for achieving reasonable accuracy is prohibitively high.

In addition to the model structure and parameters, the accuracy of PF is affected by filter design choices such as (a) the choice of the proposal distribution and (b) the choice of the resampling method [4]. This article concentrates on (a). The proposal distribution, also known as the importance distribution, is a probability distribution that is used for the generation of the new particles based on the existing particles. It is important to generate particles with high density in the relevant regions of the state space so that the particle set will be an accurate representation of the posterior probability distribution. A common choice is to use the motion model of the state as the proposal distribution; this is the bootstrap filter.

In the bootstrap filter the particles' prediction locations do not reflect the newest measurement, so if the measurement is much more precise than the prediction or conflicts with the prediction, the measurement is not taken into account properly. This results in particle degeneracy, whereby the weight concentrates to only a few particles [4]. This causes frequent resampling which introduces additional Monte Carlo error. Therefore, it is advantageous to make use of the newest measurement already in the proposal distribution [4].

In indoor positioning, the PDR distribution is typically used as both the motion model and proposal distribution, and the floor-plan is used as a measurement. That is, the particles are propagated using the PDR, and the particles that collide with a wall are given small or zero weights [2], [5]–[7]. This might lead to degeneracy especially if the PDR is low-quality, because large portions of the particles are colliding with the walls and do not contribute to the estimation.

We propose including some map information in the PF's proposal distribution. The method is based on an angular PDF (probability density function) modified from that of Kaiser et al. [8]. We distort the PDR distribution by giving more probability to the directions where the distance to the closest walls is larger. This way, fewer particles collide with the walls

H. Nurminen receives funding from Tampere University of Technology Graduate School, the Foundation of Nokia Corporation, and Tekniikan edistämisyhdistys.

M. Raitoharju works in OpenKin project that is funded by the Academy of Finland.

and more particles are modelling the most probable areas.

We test the proposed method by simulating test tracks with PDR and absolute position measurements upon real indoor floor-plans. The simulations show that the proposed method improves accuracy at least when the PDR quality is low.

In this article we first explain the angular PDF and compare it with the approach of Kaiser et al. Then, we introduce the other measurements sources. Section III explains the conventional wall collision PF and explains the novel features of our filter in detail. Section IV presents the simulation results, and Section V summarises the conclusions.

Notations: $N(\mathbf{m}, P)$ is the (multivariate) normal distribution with mean \mathbf{m} and covariance matrix P , and $N(\mathbf{x}|\mathbf{m}, P)$ is its PDF evaluated at \mathbf{x} .

II. MEASUREMENTS

We use a standard probabilistic state-space model of a time-varying state \mathbf{x}_k with associated measurements \mathbf{y}_k . The index k is the time index. A state-space model is defined by three probability distributions: the initial prior $p(\mathbf{x}_0)$, the motion model $p(\mathbf{x}_k|\mathbf{x}_{k-1})$, and the measurement model $p(\mathbf{y}_k|\mathbf{x}_k)$. Furthermore, the standard conditional independences are assumed [9, Ch. 4.1]. In this article the state vector is

$$\mathbf{x}_k = \begin{bmatrix} \mathbf{r}_k \\ \varphi_k \\ \ell_k \end{bmatrix}, \quad (1)$$

where $\mathbf{r}_k \in \mathbb{R}^2$ is the user position, $\varphi_k \in \mathbb{R}$ is the heading angle, and $\ell_k \in \mathbb{R}$ is the footstep length.

A. Pedestrian dead reckoning

Pedestrian dead reckoning (PDR) means measuring the displacement of the user from a fixed starting point. In this article it is assumed that the PDR gives reliable footstep detection and noisy measurements of the footstep length and change of heading in the horizontal plane.

In personal indoor positioning, PDR is based on inertial navigation systems (INS). An indoor positioning INS includes three-axis accelerometers and gyroscopes. The footsteps can be detected using low-pass filtered norm of acceleration [2]. The direction of gravity can also be inferred from the accelerometer data, which gives the horizontal plane, and the change of heading is then obtained by projecting the gyroscopes' angular velocity vector to the horizontal plane [10]. The footstep length can be assumed to be inversely proportional to the footstep duration with a known or fitted proportionality constant [11]. Another method for INS-based PDR would be double integration of acceleration with zero-velocity updates, but this is not reliable if the positioning device can be hand-held instead of foot-mounted.

The strengths of the PDR method in positioning are low infrastructure cost and high short-term accuracy. Its weaknesses are the need of external initial position information and its low long-term accuracy due to sensor drift. Sensor drift means that the heading obtained by integrating the gyroscope output tends to drift away from the true value because the gyroscopes always have some systematic error. Therefore, PDR with low-cost INS needs to be complemented with

additional position information such as map and/or absolute position measurements.

A conventional indoor positioning motion model that uses the PDR and no map information is

$$p(\mathbf{x}_k|\mathbf{x}_{k-1}) = N(\varphi_k|\varphi_{k-1} + \bar{\Delta}_k, q^{\bar{\Delta}}) \cdot N(\ell_k|\bar{\ell}_k, q^{\bar{\ell}}) \times N(\mathbf{r}_k|\mathbf{r}_{k-1} + \ell_{k-1} \cdot \begin{bmatrix} \cos(\varphi_k) \\ \sin(\varphi_k) \end{bmatrix}, q^{\mathbf{r}} \cdot \mathbf{I}_{2 \times 2}), \quad (2)$$

where $\bar{\Delta}_k$ is the heading change measurement (positive angle for anticlockwise) and $\bar{\ell}_k$ is the footstep length measurement, and $q^{\bar{\Delta}}$ and $q^{\bar{\ell}}$ are their variances. The matrix $q^{\mathbf{r}}\mathbf{I}$ is the covariance matrix of the user position's independent process noise; this parameter mainly affects the robustness of the PF, and it should be close to zero [7].

B. Radio network positioning

Wireless radio networks such as WLAN (wireless local area network), BLE (Bluetooth Low Energy), and UWB (ultra-wideband) can provide absolute position information, i.e. they can be used as a standalone positioning technology. However, their positioning accuracy can be relatively low especially if only the communication infrastructure WLAN without positioning-specific modifications is used. Furthermore, frequent radio scanning consumes battery power. These features make radio positioning a suitable complement for PDR: the short-term accuracy can be highly improved by the PDR, while the radio positioning is capable of giving the initial position estimate, and its quality does not degrade over time. Furthermore, radio positioning can be used for monitoring the integrity of the fusion estimate [7], [12].

For simplicity, we assume that the radio positioning system gives a position estimate with a multivariate normally distributed measurement error, i.e. the measurement model is

$$\mathbf{z}_k|\mathbf{r}_k \sim N(\mathbf{r}_k, \Sigma_k), \quad (3)$$

where \mathbf{z}_k is the 2-dimensional user position estimate, \mathbf{r}_k is the 2-dimensional user position, and Σ_k is the measurement noise covariance matrix. The position measurements can be e.g. the outcome of the coverage area positioning method [13]. It is also straightforward to inject other measurement types to a PF, such as received signal strength (RSS) of WLAN and/or BLE, time of arrival ranging of UWB, or pseudo-ranges of a satellite positioning system.

C. Map matching

In indoor positioning, map matching means using the floor-plan to exclude trajectories that cross walls or floor levels. In this article the floor-plan is a set of thin wall segments on each floor of the building. The statistical model can give a small non-zero probability for walking through a wall of the map:

$$\mathbb{P}(C_k|\mathbf{r}_k, \mathbf{r}_{k-1}) = \begin{cases} \epsilon, & C_k = \text{"a step-crossing wall in the map"} \\ 1 - \epsilon, & C_k = \text{"no step-crossing wall"} \end{cases}, \quad (4)$$

where $0 \leq \epsilon \ll 1$ holds, and \mathbb{P} denotes probability. A non-zero wall-permeability ϵ makes the estimation algorithm more

robust to small positioning errors and floor-plan errors; with $\epsilon=0$ all the particles can easily get stuck in a wrong room due to an erroneous position measurement or the map showing a wall that does not exist in reality [7]. Information on furniture or other movable objects is not used due to its changeable nature. In this work the floor-plans are HERE Venue Maps.

In addition, our algorithm uses the map information of distances from each candidate position to the closest obstacle in each direction. Formulated as a probabilistic model, this approach can be called the angular PDF. We use the angular PDF in the proposal distribution so that the more open space a particle has in a direction, the more likely the particle is moved to this direction. Thus, fewer particles will collide with the walls. The angular PDF can also be included in the motion model or the measurement likelihood.

Kaiser et al. consider a PF with a similar likelihood function in [8]. However, they use an angular PDF for particle weighting, while the particle propagation uses the PDR alone. In their nomenclature PDR model is part of the measurement likelihood while the angular PDF is called motion model. We adopt the a common convention and consider the PDR as a motion model and the angular PDF as part of either motion or measurement model depending on the PDF normalisation.

Kaiser et al. argue that the angular PDF helps in balancing between open areas and more narrow spaces [8]. They demonstrate how a particle subcloud in a narrow corridor will eventually disappear in the conventional PF due to wall collisions if there is another subcloud in a more open area, e.g. outdoors. The approach of [8] indeed gives more weight to areas where the PDR track is a close match to the building layout, i.e. the PDR direction is one of few directions allowed by the map, while open areas are underweighted. This feature is justified in some cases as demonstrated in [8], but results in erroneous outcomes in other cases. For example, when the user walks straight, narrow corridors are favoured over wider ones, which we do not consider a realistic model in general. Particle weighting with a likelihood that is not used in the proposal distribution can also result in more frequent resampling.

In [8], the measure of open space in a direction is the distance to certain contour plots of the gas diffusion distribution or to the closest wall, whichever is smaller. That is, the current waypoint (a point of a grid) is used as a source for a free gas diffusion and full wall absorption model. Instead of the diffusion contour distance, we use an increasing function of the distance to the closest wall. We chose this approach mainly to reduce computational burden and to make the implementation simpler; in our approach one needs to implement the crossing point of two line segments, while the diffusion algorithm includes that and other computations in addition. The gas diffusion model can be linked to the diffusion of probability, but its use as part of the likelihood is still heuristic, and [8] does not give any justification to the gas diffusion model compared to other models. Furthermore, the diffusion approach results in unwanted phenomena such as the fact that narrow long corridors are weighted less than wide long corridors because the gas-absorbing walls are closer.

Due to high computational requirements, we compute the angular PDFs offline in a server. We discretise the area into a regular square grid with a 0.5 m spacing. From each grid point we compute the distance to the closest wall in each direction with a 5-degree discretisation interval. If the distance is more than 10 m, we set the distance to 10 m because we assume that differences beyond that do not affect the heading distribution. Because the grid is regular, the grid point coordinates need not be stored and the grid density does not affect critically the computational heaviness of particle-grid point matching. The database size is the same as in [8].

If floor-plan is not available for an area, the angular PDF becomes uniform giving the standard PF. PF can also be transformed into a computationally faster KF by computing the mean and covariance matrix of the KF state variables. Furthermore, KF can be transformed into a PF by sampling from the KF distribution when a map is again available.

III. PARTICLE FILTERING SOLUTION

This section first explains the conventional wall collision PF and then presents our novel modifications.

A. Wall collision particle filter

The particle filter (PF) is an importance sampling approximation of the Bayesian filter for the state-space model [3]. Let \mathbf{x}_k^i denote the state of the i th particle at the k th time instant, W_k^i its weight, and N the number of particles. Initially, the particles are equal-weighted samples from the initial prior $p(\mathbf{x}_0)$. At each time instant, they are propagated by generating new samples from the proposal distribution $q_k(\mathbf{x}_k|\mathbf{x}_{0:k-1}^i, \mathbf{y}_{1:k})$, where the conditioning is on all the previous states of the particle and all the measurements up to and including the newest measurement. The proposal distribution can be chosen freely given that one can easily sample from it and that its support covers the posterior distribution's support. However, the PF algorithm will be the more efficient in estimation accuracy the closer the proposal distribution is to the actual posterior, and the distribution $p(\mathbf{x}_k|\mathbf{x}_{k-1}^i, \mathbf{y}_k)$ is the optimal proposal in the sense that it minimises the variance of the weight W_k^i given $\mathbf{x}_{0:k-1}^i$ and $\mathbf{y}_{1:k}$ [14].

The particle weights are affected by the motion model, measurement likelihood, and proposal distribution. The weight update of the wall collision PF is

$$\widetilde{W}_k^i = \frac{p(\mathbf{z}_k|\mathbf{x}_k^i) \mathbb{P}(C_k|\mathbf{x}_k^i, \mathbf{x}_{k-1}^i) p(\mathbf{x}_k^i|\mathbf{x}_{k-1}^i)}{q(\mathbf{x}_k^i|\mathbf{x}_{0:k-1}^i, \mathbf{y}_{1:k})} \cdot W_{k-1}^i, \quad (5)$$

where \mathbf{z}_k is the absolute position measurement and $\mathbf{y}_{1:k}$ includes absolute position, map information, and possible other types of measurements. The normalisation factor of the posterior is not required because the normalisation to unity

$$W_k^i = \widetilde{W}_k^i / \sum_{j=1}^{N_p} \widetilde{W}_k^j \quad (6)$$

tends to approximate it well [9, Ch. 7.2].

The resampling step ensures that weight does not eventually concentrate to one or few particles. In this article, the particles are resampled after the measurement update whenever

Algorithm 1 Computation of the wall distances

Input: grid points $\mathbf{g}_1:N_{\text{grid points}}$, angle discretisation $N_\alpha = 72$, $\alpha = \{0^\circ, 5^\circ, 10^\circ, \dots, 355^\circ\} \cdot \pi/180^\circ$, walls
Output: matrix of wall distances $S \in \mathbb{R}^{N_{\text{grid points}} \times N_\alpha}$
for $m \in \{1 : N_{\text{grid points}}\}$ **do**
 for $j \in \{1 : N_\alpha\}$ **do**
 for $n \in \{\text{all walls within 10 m radius}\}$ **do**
 $\ell :=$ line segment $(\mathbf{g}_m, \mathbf{g}_m + (10 \text{ m}) \cdot [\cos(\alpha_j)])$
 if ℓ and wall n cross **then**
 $\mathbf{r}^* :=$ crossing point of ℓ and wall n
 $\mathbf{d}_n := \|\mathbf{r}^* - \mathbf{g}_m\|$
 else
 $\mathbf{d}_n := 10 \text{ m}$
 end if
 end for
 $[S]_{m,j} := \min_n \mathbf{d}_n$
 end for
end for

$1/\sum_{i=1}^{N_p} (W_k^i)^2 < 0.1 \cdot N_p$, which is the standard approach based on the effective particle number [3, Ch. 3.3]. In the tests, the multinomial resampling is used, where the new particles are generated with replacement from the discrete distribution defined by the previous particle states and weights [15].

As a fourth step, the PF's integrity is monitored by running a fallback KF in parallel with the PF [7], [12]. This monitor detects when the whole particle cloud gets stuck behind walls in a wrong area, and restarts the PF. This article uses the PDR-Kalman of Raitoharju et al. [12] that uses a linear motion model. The fallback KF uses the PDR and absolute position measurements, but it is independent of the floor-plan and particles to avoid getting stuck.

The conventional wall collision PF such as Algorithm 1 of [7] is a bootstrap PF, i.e. the motion model is used as the proposal distribution, so the term $p(\mathbf{x}_k^i | \mathbf{x}_{k-1}^i) / q(\mathbf{x}_k^i | \mathbf{x}_{0:k-1}^i, \mathbf{y}_{1:k})$ vanishes from (5). This choice can be inefficient when the INS has high noise level and the positioning area is dense in walls, i.e. the process noise variance is large compared to the measurement noise variance.

B. Particle generation using PDR and floor-plan

This subsection explains a novel proposal distribution that includes some map information already in the particle propagation phase. We propose using an angular motion model modified from the angular PDF of [8] to particle propagation.

In the offline phase, we begin by defining a regular square grid for the building. For each grid point and for each direction with a fixed angle discretisation, we compute distances to the closest wall. These are stored in a database for the online phase. The details are given in Algorithm 1.

In the PF's particle propagation phase we choose the closest grid point m^i to each particle, which is straightforward to find because the grid is a regular square grid. It would be justified to limit the grid point search to the particle's room, but this could be computationally expensive, so we leave this for future

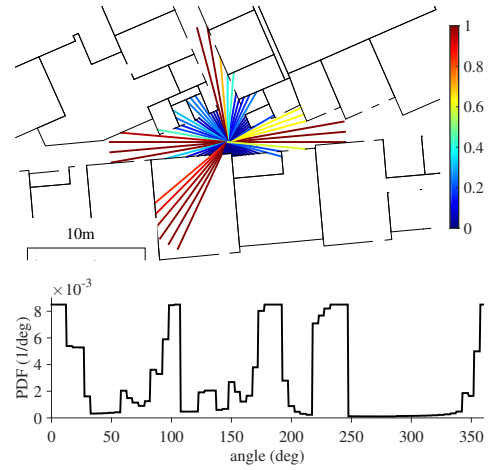


Fig. 1. The proposed angular PDF. In the upper figure the lengths of the radial line segments represent the wall distances $[S]_{m,j}$, while the colours represent the angular PDF (9) with 0.7 m footprint length.

research and assume that the wall collision weighting corrects errors caused by choosing the grid point from a wrong room. The wall distances of the chosen grid point are converted into the angular PDF using a monotonically increasing function. We use the logistic function and normalisation to unity

$$\tilde{s}_{m^i}(\alpha_j) = \frac{1}{1 + 99 \exp(-0.8 \cdot ([S]_{m^i,j} - \ell_k^i))}, \quad (7)$$

$$s_{m^i}(\alpha_j) = \tilde{s}_{m^i}(\alpha_j) / \sum_{j=1}^{N_\alpha} \tilde{s}_{m^i}(\alpha_j), \quad (8)$$

which give small non-zero weights to distances shorter than the footprint length and a small slope with distances of several meters. The result is the piecewise-constant PDF

$$p_\alpha(\varphi_k | \mathbf{r}_{k-1}^i, \ell_k^i) = \frac{N_\alpha}{2\pi} \sum_{j=1}^{N_\alpha} s_{m^i}(\alpha_j) \cdot I_{[\alpha_j - \pi/N_\alpha, \alpha_j + \pi/N_\alpha]}(\varphi_k), \quad (9)$$

where $I_S(x)$ is the indicator function for set S . An example of an angular PDF is given in Fig. 1.

We want the proposal distribution to be the product of the floor-plan-based and PDR-based PDFs. Thus, our novel proposal distribution for the user's heading is

$$q(\varphi_k | \mathbf{r}_{k-1}^i, \varphi_{k-1}^i, \ell_k^i, \bar{\Delta}_k, \text{map}) = \frac{1}{Z^i} p_\alpha(\varphi_k | \mathbf{r}_{k-1}^i, \ell_k^i) \mathcal{N}(\varphi_k | \varphi_{k-1}^i + \bar{\Delta}_k, q^{\bar{\Delta}}) \quad (10)$$

$$= \frac{1}{Z^i} \sum_{j=1}^{N_\alpha} w_j^i \mathcal{N}_{[\alpha_j - \pi/N_\alpha, \alpha_j + \pi/N_\alpha]}(\varphi_k | \varphi_{k-1}^i + \bar{\Delta}_k, q^{\bar{\Delta}}), \quad (11)$$

where $\mathcal{N}_{[a,b]}$ is normal distribution truncated to interval $[a,b]$

$$\mathcal{N}_{[a,b]}(x | \mu, \sigma^2) = \frac{1}{\Phi((b-\mu)/\sigma) - \Phi((a-\mu)/\sigma)} \mathcal{N}(x | \mu, \sigma^2) \cdot I_{[a,b]}(x),$$

and

$$w_j^i = \frac{N_\alpha}{2\pi} \cdot s_{m^i}(\alpha_j) \cdot [\Phi(\Delta^<(\alpha_j + \pi/N_\alpha, \varphi_{k-1}^i + \bar{\Delta}_k) / (q^{\bar{\Delta}})^{\frac{1}{2}}) - \Phi(\Delta^<(\alpha_j - \pi/N_\alpha, \varphi_{k-1}^i + \bar{\Delta}_k) / (q^{\bar{\Delta}})^{\frac{1}{2}})], \quad (12)$$

$$Z^i = \sum_{j=1}^{N_\alpha} w_j^i, \quad (13)$$

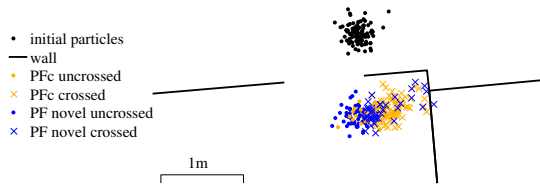


Fig. 2. Particle propagation with conventional PF (PFc) and the proposed method (PF novel) with heading $\varphi \sim \mathcal{N}(290^\circ, (10^\circ)^2)$. Map guides 60% of PF novel particles through a door, while only 20% of PFc particles survive.

$\Delta_{\angle}(\alpha, \beta)$ being the difference angle $\alpha - \beta$ translated by a multiple of 2π to the interval $(-\pi, \pi]$, and $\Phi(x)$ being the cumulative distribution function (CDF) of the standard normal distribution. If the heading change measurement noise follows a non-normal distribution, Φ can be replaced by the appropriate CDF.

Sampling from the distribution (11) is straightforward. First, one generates an index j^i by sampling from the categorical distribution $\text{cat}(w_1^i/Z^i, \dots, w_{N_\alpha}^i/Z^i)$, i.e. the discrete distribution of $\{1, 2, \dots, N_\alpha\}$ with the probabilities $\{w_1^i/Z^i, \dots, w_{N_\alpha}^i/Z^i\}$. Then, the sample of (11) is generated from $N_{[\alpha_{j^i} - \pi/N_\alpha, \alpha_{j^i} + \pi/N_\alpha]}(\varphi_{k-1}^i + \bar{\Delta}_k, q^{\bar{\Delta}})$, for which efficient methods exist, see e.g. [16]. Fig. 2 shows an example where the novel proposal distribution guides most of the particles through a door while few particles survive with the conventional PDR-only proposal distribution.

Our novel proposal distribution could also be used without any PDR. However, in this case a graph-based map matching method might be more efficient unless the absolute position measurements are very accurate and are made frequently [17].

By modifying the weighting function (7), the proposal distribution could be tuned so that none of the particles would collide with walls (given $q^F = 0$). However, floor-plan errors would not then be modelled, and wall constraints would not be used as measurements that remove particle subclouds where PDR contradicts with the map. Thus, we allow some wall collisions. Notice that the more accurate the PDR, the less influence the map-based angular PDF has. With very accurate PDR few particles should collide with walls anyway.

C. Angular PDF in motion model and/or likelihood

The floor-plan based proposal distribution inspires three PF algorithms: the angular PDF is used only in the proposal distribution, the angular PDF is included in both motion model and proposal distribution, or it is included in measurement likelihood and proposal distribution. The three algorithms differ in the particle weight update formula. A detailed description of the three PFs is presented in Algorithm 2.

PF1: If the angular PDF is used only in the proposal, the proposal PDF and motion model PDF are different, so they do not cancel each other in (5). The update becomes

$$\widetilde{W}_k^i = p(\mathbf{z}_k | \mathbf{x}_k^i) \mathbb{P}(C_k | \mathbf{x}_k^i, \mathbf{x}_{k-1}^i) \frac{Z^i}{s_{m^i}(\alpha_{j^i})} \cdot W_{k-1}^i, \quad (14)$$

where j^i is the angle discretisation index generated for the i th particle. The resulting PF is a solution to the same problem as

the conventional wall collision PF, but the particles will collide with the walls less frequently due to the modified proposal distribution. However, the difference in proposal and motion model can again increase the resampling rate.

PF2: If the angular PDF is used in both proposal distribution and motion model, the term $N(\varphi_k | \varphi_{k-1} + \bar{\Delta}_k, q^{\bar{\Delta}})$ in (2) is replaced by the distribution of (11), so the proposal and motion model cancel out each other in the weight update (5) which then simplifies to

$$\widetilde{W}_k^i = p(\mathbf{z}_k | \mathbf{x}_k^i) \mathbb{P}(C_k | \mathbf{x}_k^i, \mathbf{x}_{k-1}^i) \cdot W_{k-1}^i. \quad (15)$$

This weight update is similar to that of the conventional wall collision PF. However, the motion model is different due to different particle propagation. The proposal PDF cancels out completely in the weight update, so this should provide the lowest resampling rate of the proposed three algorithms. This motion model should be advantageous when the PDR is inaccurate, i.e. $q^{\bar{\Delta}}$ is large, because the probability is not spread to random directions but more probability will be assigned to corridor and open space directions, which can be considered more likely. A possible drawback is that the influence of the map measurements is reduced: particles of wrong areas are not eliminated so often by wall collisions, but the filter relies more on the absolute position measurements.

PF3: If the angular PDF is used in both proposal distribution and measurement likelihood, the proposal distribution's normalisation factor does not cancel out in (5), so the weight update is

$$\widetilde{W}_k^i = p(\mathbf{z}_k | \mathbf{x}_k^i) \mathbb{P}(C_k | \mathbf{x}_k^i, \mathbf{x}_{k-1}^i) \cdot Z^i \cdot W_{k-1}^i. \quad (16)$$

This approach is based on the same motion and measurement models as the method of [8]. Compared to PF2, the proposal distribution's normalisation factor Z^i gives more weight to the particles where the heading matches best with the map.

A major motivation of Kaiser et al. is the scenario where there is imprecise PDR and a bimodal particle cloud with one subcloud in a narrow corridor and another subcloud in open space [8]. In PF3 all the weight will eventually concentrate in the corridor. In PF1 the open space will eventually be more probable, but the proposal distribution improves the estimation in narrow corridors so that the corridor subcloud will die out slower than in the conventional wall collision PF. The approach PF2 gives more weight to the corridor than PF1 but the weight is not moved from open space to corridor. In summary, only PF3 meets the requirement that in multimodal situations the weight should eventually concentrate to narrow corridors, but PF1 and PF2 attempt to make the modelling of corridors more accurate and let the absolute positioning decide in cases with multimodal distributions.

IV. TESTING

A. Simulation setting

We test the proposed algorithms with simulated indoor positioning data. The tests were implemented with MATLAB. We used the floor-plan of a campus building of Tampere

Algorithm 2 PF with map & PDR based proposal distribution

Input: prior $p(\mathbf{x}_0)$; number of particles N_p , PDR $\{\bar{\Delta}_k, \bar{\ell}_k\}$ and position meas. \mathbf{z}_k , $k \in \{1, \dots\}$; map; angular PDF $s_m(\alpha_j)$

Output: position estimate $\hat{\mathbf{r}}_k$ and covariance matrix $\hat{\Sigma}_k$

- 1) For each $i = \{1, \dots, N_p\}$ set $W_0^i := \frac{1}{N_p}$ and generate $\mathbf{x}_0^i \leftarrow p(\mathbf{x}_0)$. Set the time index $k := 1$.
- 2) If no footstep is detected at time index k , go to step 5. Otherwise, find the closest grid point m^i for each $i = \{1, \dots, N_p\}$, and generate

$$\ell_k^i \leftarrow N(\bar{\ell}_k, q^{\bar{\ell}})$$

$$j^i \leftarrow \text{cat}(w_1^i/Z^i, \dots, w_{N_\alpha}^i/Z^i), Z^i = \sum_{j=1}^{N_\alpha} w_j^i$$

$$\varphi_k^i \leftarrow N_{[\alpha_{j^i} - \pi/N_\alpha, \alpha_{j^i} + \pi/N_\alpha]}(\varphi_{k-1}^i + \bar{\Delta}_k, q^{\bar{\Delta}})$$

$$\mathbf{r}_k^i \leftarrow N(\mathbf{r}_{k-1}^i + \ell_k^i \cdot \begin{bmatrix} \cos(\varphi_k^i) \\ \sin(\varphi_k^i) \end{bmatrix}, q^{\mathbf{r}} \cdot \mathbf{I}_{2 \times 2})$$

- 3) Perform angular PDF weighting $\widetilde{W}_k^i := \mathcal{W}_\alpha^i \cdot W_{k-1}^i$ with
 - PF1: $\mathcal{W}_\alpha^i = Z^i / s_{m^i}(\alpha_{j^i})$
 - PF2: $\mathcal{W}_\alpha^i = 1$
 - PF3: $\mathcal{W}_\alpha^i = Z^i$
 - 4) Set $\widetilde{W}_k^i := \frac{\epsilon}{1-\epsilon} \widetilde{W}_k^i$ for all i such that there is a wall between \mathbf{r}_{k-1}^i and \mathbf{r}_k^i , where ϵ is defined in (4).
 - 5) Perform integrity monitoring using the PDR-Kalman. If re-initialised, go to step 7.
 - 6) If no absolute position measurement is obtained at time index k , go to step 7. Otherwise, set $\widetilde{W}_k^i := N(\mathbf{r}_k^i | \mathbf{z}_k, \Sigma_k) \cdot \widetilde{W}_k^i$ for each $i \in \{1, 2, \dots, N_p\}$.
 - 7) Normalise the weights by $W_k^i := \widetilde{W}_k^i / \sum_{j=1}^{N_p} \widetilde{W}_k^j$ for each $i \in \{1, 2, \dots, N_p\}$.
 - 8) $\hat{\mathbf{r}}_k := \sum_{i=1}^{N_p} W_k^i \mathbf{r}_k^i$, $\hat{\Sigma}_k := \sum_{i=1}^{N_p} W_k^i (\mathbf{r}_k^i - \hat{\mathbf{r}}_k)(\mathbf{r}_k^i - \hat{\mathbf{r}}_k)^T$
 - 9) If $1 / \sum_{i=1}^{N_p} (W_k^i)^2 < 0.1 \cdot N_p$, resample, and set $W_k^i := 1/N_p$. Set $k := k + 1$, and go to step 2.
-

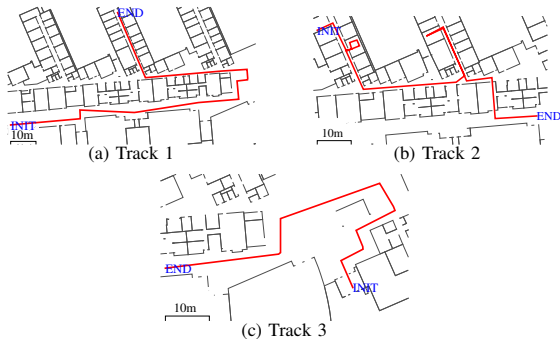


Fig. 3. The test tracks. Track 1 tests behaviour in corridors, track 2 tests doors and rooms, and track 3 tests open space.

University of Technology. We designed three different tracks to test different properties of the algorithms. The tracks are depicted in Fig. 3. Track 1 tests the algorithms' behaviours in corridors, track 2 tests doors and rooms, while track 3 tests open spaces and transition from an open space to a corridor.

The test tracks' paths were defined by hand, but the footstep

lengths ℓ_k were simulated from the model

$$v_0 \sim N(0, 0.2718^2), \quad (17)$$

$$\begin{bmatrix} \ell_k \\ v_k \end{bmatrix} \sim N \left(\begin{bmatrix} 0.7 + 0.9748v_{k-1} \\ 0.95v_{k-1} \end{bmatrix}, \begin{bmatrix} 0.3208 & 0.4751 \\ 0.4751 & 0.9504 \end{bmatrix} \right) \quad (18)$$

This model guarantees that the marginal distribution of each ℓ_k is $N(0.7, 0.2718^2)$. The step detection was assumed perfect, and the PDR measurements were generated by

$$\bar{\ell}_k \sim N(\|\mathbf{r}_k - \mathbf{r}_{k-1}\|, (0.7 \text{ m} \cdot 2^\circ \frac{\pi}{180^\circ})^2) \quad (19)$$

$$\bar{\Delta}_k \sim N(\Delta_k - 0.3^\circ \frac{\pi}{180^\circ}, q^{\bar{\Delta}} - (0.3^\circ \frac{\pi}{180^\circ})^2), \quad (20)$$

$$\Delta_k = \Delta^\angle(\text{atan}_2([\mathbf{r}_k - \mathbf{r}_{k-1}]_2, [\mathbf{r}_k - \mathbf{r}_{k-1}]_1), \text{atan}_2([\mathbf{r}_{k-1} - \mathbf{r}_{k-2}]_2, [\mathbf{r}_{k-1} - \mathbf{r}_{k-2}]_1)).$$

The model includes a gyro bias of -0.3° per step. The absolute position measurements were generated by

$$\mathbf{z}_k \sim N(\mathbf{r}_k, (4 \text{ m})^2 \cdot \mathbf{I}_{2 \times 2}), \quad (21)$$

and the measurements were received every 20 steps.

B. Filter details

The compared methods are the PDR Kalman filter (KF), the conventional wall collision PF (PFc), the wall collision PF with the conventional (PDR-based) proposal distribution and angular PDF likelihood weighting (PFw), the PF with the novel proposal distribution (PF1), the PF with the novel proposal distribution and the angular PDF included in the motion model (PF2), and the PF with the novel proposal distribution and the angular PDF included in the measurement likelihood (PF3).

The filters are given the correct initial position with covariance matrix $\mathbf{I}_{2 \times 2}$ and the correct initial heading with variance $(3^\circ)^2$. In a real scenario, if the initial state were unknown, the KF could be used in the beginning to improve the initial prior of the PF [12]. The KF is based on the motion model

$$\begin{bmatrix} \mathbf{r}_k \\ \mathbf{v}_k \end{bmatrix} \mid \begin{bmatrix} \mathbf{r}_{k-1} \\ \mathbf{v}_{k-1} \end{bmatrix} \sim N \left(\begin{bmatrix} \mathbf{I} & \mathbf{R}_k \\ \mathbf{O} & \mathbf{R}_k \end{bmatrix} \begin{bmatrix} \mathbf{r}_{k-1} \\ \mathbf{v}_{k-1} \end{bmatrix}, \begin{bmatrix} q^{\mathbf{r}} \cdot \mathbf{I} & \mathbf{O} \\ \mathbf{O} & \sigma_v^2 \cdot \mathbf{I} \end{bmatrix} \right), \quad (22)$$

where \mathbf{r} is user position, \mathbf{v} is step vector, $q^{\mathbf{r}} = (0.01 \text{ m})^2$, and

$$\mathbf{R}_k = \begin{bmatrix} \cos \bar{\Delta}_k & -\sin \bar{\Delta}_k \\ \sin \bar{\Delta}_k & \cos \bar{\Delta}_k \end{bmatrix}, \sigma_v^2 = \max\left\{ \left(\frac{\pi}{90}\right)^2, q^{\bar{\Delta}} \right\} \cdot (0.7 \text{ m})^2.$$

The KF is thus a version of the PDR-Kalman of [12]. Notice that the KF uses neither footstep length nor map measurements. The same KF is also used as a fallback of the PFs, so that half of the particles are re-initialised if none of the non-zero-weighted particles are in the 99% probability ellipse of the KF-posterior, similarly to [7].

For robustness, the PFs' propagation step adds independent noise to position with the variance parameter $q^{\mathbf{r}} = (0.01 \text{ m})^2$. The PFs do not take the gyro bias into account, i.e. the PDR model is $\varphi_k | \varphi_{k-1} \sim N(\varphi_{k-1} + \bar{\Delta}_k, q^{\bar{\Delta}})$. The wall collision checking of the particles is implemented so that each square of a regular grid is assigned with the walls that cross this square, and only the grid squares that are crossed by

the particle trajectory are checked. This is important for the computational efficiency [2]. If a particle crosses a wall, its weight is multiplied by $\frac{\epsilon}{1-\epsilon} = 10^{-4}$.

C. Results and discussion

Fig. 4 shows boxplots of the simulated empirical distributions of the root-mean-square-errors (RMSE) of the filters for the three tracks, for three different values of the gyro noise parameter q^{Δ} , and for different numbers of particles N_p . The boxplots show the 5%, 25%, 50%, 75%, and 95% quantiles. The results are based on 100 Monte Carlo replications.

Fig. 4 shows that PF2 has the lowest errors of the novel filters. PF2 converges to the same or slightly better RMSE than the conventional wall collision filter PFc, but with small numbers of particles N_p PF2 is significantly more accurate in corridor tracks 1 and 2 and has similar accuracy in the open space track 3. This can be explained by the fact that the novel proposal distribution makes the filter more efficient in corridors and small rooms. The advantage of PF2 is also clearer when PDR is imprecise, i.e. when q^{Δ} is large, which was expectable because the map measurements have a fixed resolution: when PDR is very precise, the map does not help.

PF1 converges to the same results as PFc, but with noisy PDR and low N_p PF1 outperforms PFc. PFw and PF3 are also based on the same model, and PF3 gives slightly better results with small N_p . Notice that the angular PDF as a part of the measurement likelihood in PFw and PF3 behaves as expected: the accuracy is high on track 1 which consists of corridors, but low on tracks 2 (doors, rooms) and 3 (open space).

Fig. 5 shows the resampling rates of the algorithms, i.e. the number of resamplings divided by the number of footsteps. The results show that the proposed method PF2 has clearly the lowest resampling rate especially when the PDR is imprecise and when the track contains doors and narrow corridors (track 2). Low resampling rate indicates reduced particle degeneracy, which is one explanation for the good performance of PF2.

Based on this simulation, the PF with the novel proposal distribution and angular PDF-affected motion model provides the best accuracy with a small number of particles. Notice that the novel filters require more offline and more online computation per particle as well as a larger map database than the conventional filter PFc. However, the differences in online computation are small compared to the differences in the required N_p ; in our MATLAB implementation the online computational requirements of PF1, PF2, and PF3 were roughly 50% higher than that of the PFc with the same N_p , and roughly 15% higher than that of the PFw.

V. CONCLUSIONS

We have presented a novel floor-plan and PDR based proposal distribution for indoor positioning particle filtering. Three versions of the proposed particle filter were compared by computer simulations with the conventional wall collision particle filter and with the particle filter that uses the angular PDF only for particle weighting. Our simulations showed that using floor-plan information in the particle filter's proposal

distribution improves accuracy and reduces particle degeneracy especially when computational resources are limited and PDR measurements are noisy. Furthermore, our simulations showed that the angular PDF should also be included in the motion model so that motion model and proposal distribution become the same distributions.

An important topic for future work is generalising the proposed model to multifloor buildings. Another open problem is how to compress the size of the map database: the proposed method requires a grid where each grid point contains an offline-computed discrete distribution with 72 parameters. This might be reduced for example by fitting a continuous distribution to each grid point instead of the discrete distribution.

REFERENCES

- [1] J. Liu, R. Chen, L. Pei, R. Guinness, and H. Kuusniemi, "A hybrid smartphone indoor positioning solution for mobile LBS," *Sensors*, vol. 12, no. 12, pp. 17 208–17 233, December 2012.
- [2] H. Leppäkoski, J. Collin, and J. Takala, "Pedestrian navigation based on inertial sensors, indoor map, and WLAN signals," *Journal of Signal Processing Systems*, vol. 71, no. 3, pp. 287–296, June 2013.
- [3] B. Ristic, S. Arulampalam, and N. Gordon, *Beyond the Kalman Filter: Particle Filters for Tracking Applications*. Boston, London: Artech House, 2004.
- [4] F. Gustafsson, "Particle filter theory and practice with positioning applications," *IEEE Aerospace and Electronic Systems Magazine*, vol. 25, no. 7, pp. 53–82, July 2010.
- [5] F. Evennou, F. Marx, and E. Novakov, "Map-aided indoor mobile positioning system using particle filter," in *IEEE Wireless Communications and Networking Conference (WCNC)*, March 2005, pp. 2490–2494.
- [6] Widyawan, M. Klepal, and S. Beaugard, "A Backtracking Particle Filter for Fusing Building Plans with PDR Displacement Estimates," in *5th Workshop on Positioning, Navigation and Communication (WPNC)*, 2008, pp. 207–212.
- [7] H. Nurminen, A. Ristimäki, S. Ali-Löytty, and R. Piché, "Particle filter and smoother for indoor localization," in *International Conference on Indoor Positioning and Indoor Navigation (IPIN)*, October 2013, pp. 137–146.
- [8] S. Kaiser, M. Khider, and P. Robertson, "A human motion model based on maps for navigation systems," *EURASIP Journal on Wireless Communications and Networking*, vol. 2011, no. 60, 2011.
- [9] S. Särkkä, *Bayesian Filtering and Smoothing*. Cambridge, UK: Cambridge University Press, 2013.
- [10] J. Collin, O. Mezentsev, and G. Lachapelle, "Indoor positioning system using accelerometry and high accuracy heading sensors," in *GPS/GNSS 2003 Conference*, September 2003.
- [11] W. Chen, R. Chen, Y. Chen, H. Kuusniemi, and J. Wang, "An effective pedestrian dead reckoning algorithm using a unified heading error model," in *2010 IEEE/ION Position Location and Navigation Symposium (PLANS)*, May 2010, pp. 340–347.
- [12] M. Raitoharju, H. Nurminen, and R. Piché, "Kalman filter with a linear state model for PDR+WLAN positioning and its application to assisting a particle filter," *EURASIP Journal on Advances in Signal Processing*, vol. 1, no. 33, December 2015.
- [13] L. Koski, T. Perälä, and R. Piché, "Indoor positioning using WLAN coverage area estimates," in *2010 International Conference on Indoor Positioning and Indoor Navigation (IPIN)*, September 2010.
- [14] A. Doucet, S. Godsill, and C. Andrieu, "On sequential Monte Carlo sampling methods for Bayesian filtering," *Statistics and Computing*, vol. 10, pp. 197–208, 2000.
- [15] J. D. Hol, T. B. Schön, and F. Gustafsson, "On resampling algorithms for particle filters," in *IEEE Nonlinear Statistical Signal Processing Workshop (NSSPW)*, September 2006, pp. 79–82.
- [16] N. Chopin, "Fast simulation of truncated Gaussian distributions," *Statistics and Computing*, vol. 21, no. 2, pp. 275–288, April 2011.
- [17] M. Koivisto, H. Nurminen, S. Ali-Löytty, and R. Piché, "Graph-based map matching for indoor positioning," in *10th International Conference on Information, Communications and Signal Processing (ICICSP)*, December 2015.

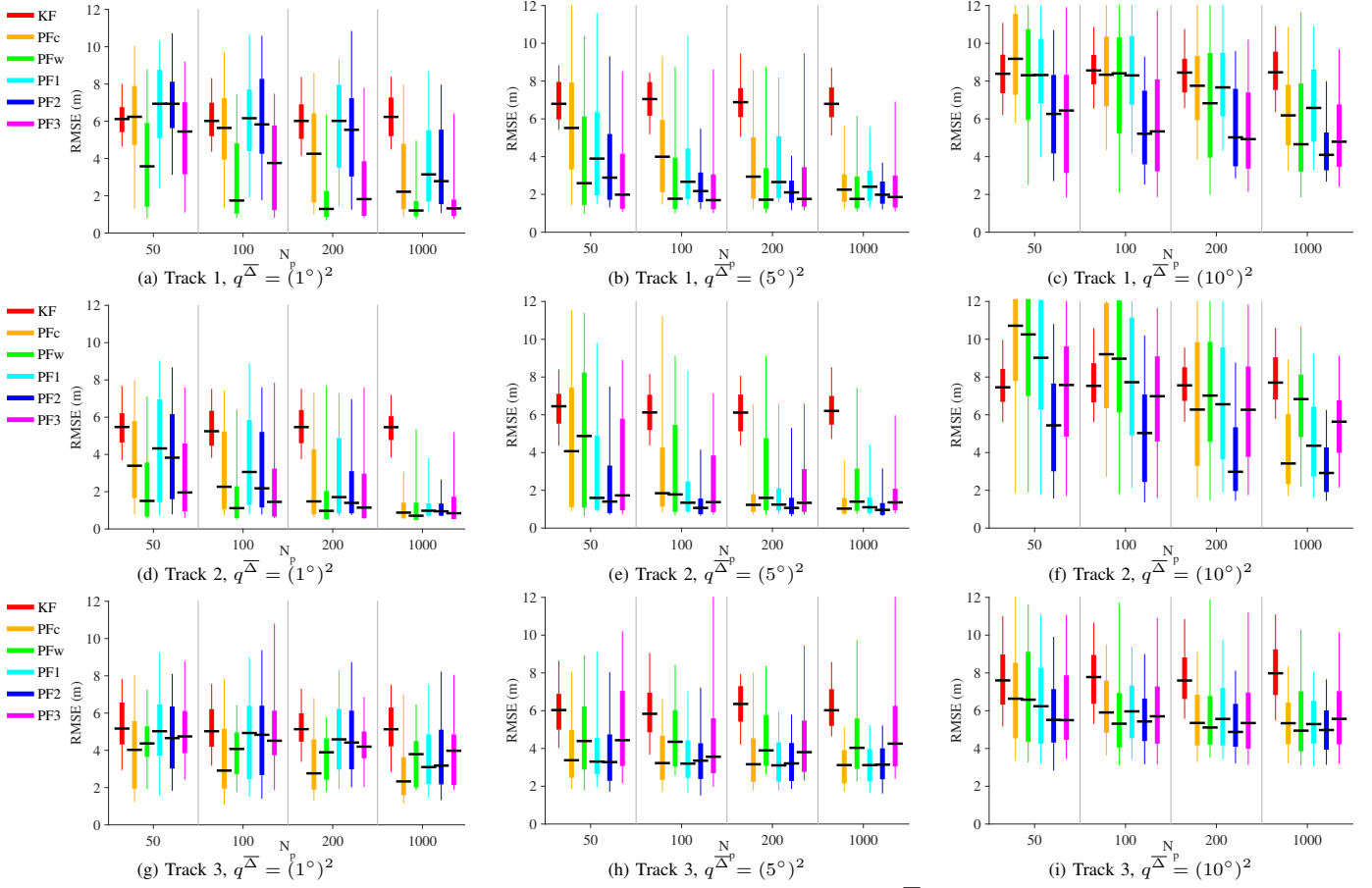


Fig. 4. Simulated RMSE distributions for three test tracks and different values of gyro noise variance q^{Δ} and the number of particles N_p . PF2 outperforms the others especially when the number of particles N_p is low, q^{Δ} is large, and the track contains narrow corridors and doors (track 2).

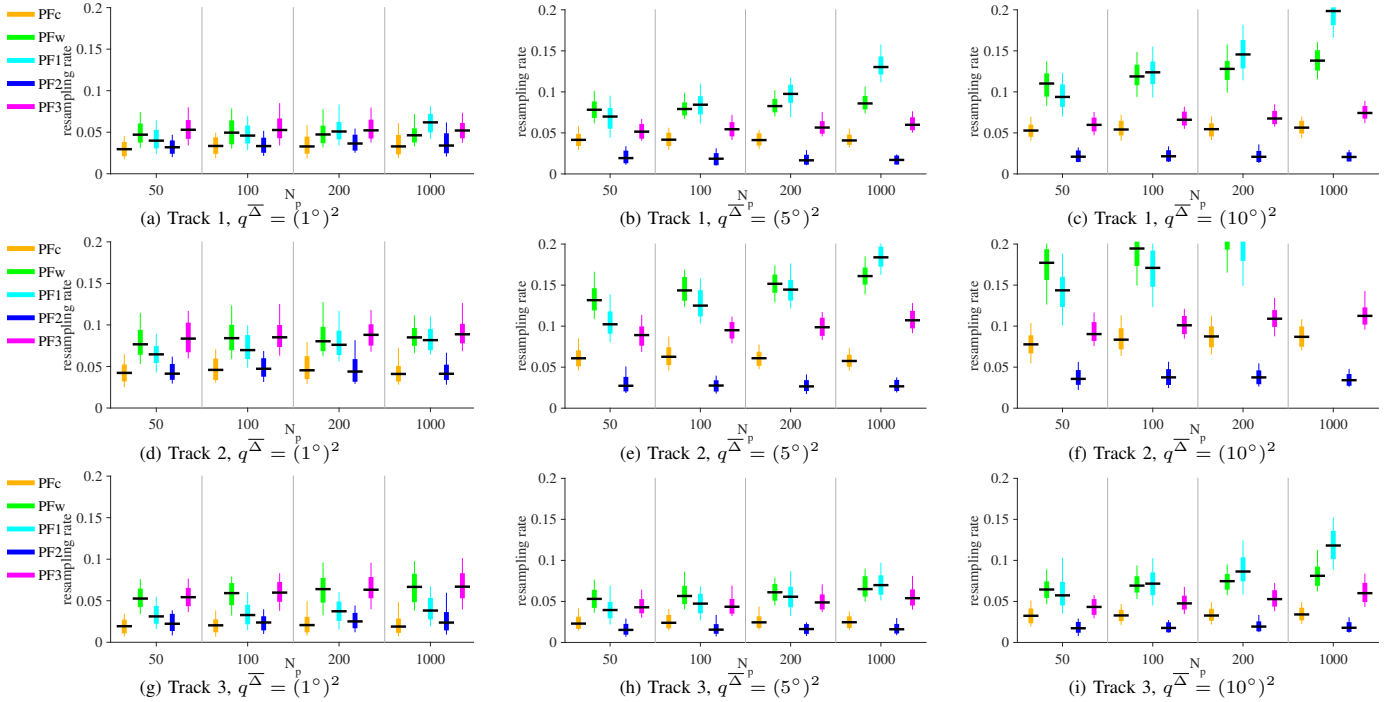


Fig. 5. Simulated resampling rate distributions. PF2 has the lowest resampling rate, which reduces Monte Carlo error and thus explains good performance.